separations

MDPI

Article

Lanthanum Diffusion in Fluorapatite at 400 °C, 50 MPa and 4–16 wt %

Xiqiang Liu [1,2], Hui Zhang [1,*] and Yunlong Liu [3]

[1] Key Laboratory of High-Temperature and High-Pressure Study of The Earth's Interior, Institute of Geochemistry, Chinese Academy of Sciences, Guiyang 550081, China; liuxiqiang@mail.gyig.ac.cn
[2] University of Chinese Academy of Sciences, Beijing 100049, China
[3] The School of Management Science, Guizhou University of Finance and Economics, Guiyang 550025, China; lyl007tt@163.com
* Correspondence: zhanghui@mail.gyig.ac.cn; Tel.: +86-139-8543-4327

Abstract: Apatite is an important carrier of rare earth elements (REEs) and phosphorite is a potential REEs resource. However, the influence of hydrothermal fluids on the migration and enrichment of REE in apatite remains controversial. The experimental study of the interaction between REE-bearing fluid and apatite is one of the essential ways to understand the chemical behavior of rare earth elements in apatite. In this study, we conducted the fluid–mineral reaction experimental study (at 400 °C, 50 MPa and 4–16 wt %) between high lanthanum (La) content hydrothermal solution and low REE content to reveal the influence of different salinities on the diffusion of rare earth elements in fluorapatite. Based on in situ geochemical analyses of experimental products, we show that the diffusion coefficients of La in fluorapatite are between 3.24×10^{-15} and 5.88×10^{-15} m^2/s. The salinity of the fluid has a great influence on the diffusion coefficient, with the increase of salinity, the diffusion coefficient increase.

Keywords: water–mineral reaction; fluorapatite; lanthanum; diffusion

Citation: Liu, X.; Zhang, H.; Liu, Y. Lanthanum Diffusion in Fluorapatite at 400 °C, 50 MPa and 4–16 wt %. *Separations* **2021**, *8*, 72. https://doi.org/10.3390/separations8060072

Academic Editor: Artem Gelis

Received: 1 May 2021
Accepted: 19 May 2021
Published: 21 May 2021

1. Introduction

Rare earth elements (REEs, include yttrium) in natural solutions have attracted much attention due to the importance of chemical tracers for natural fluid–rock (mineral) reactions [1]. The composition of rare earth elements in geological fluids is affected by ion complexation, recrystallization and selective adsorption of minerals [2]. The distribution pattern of rare earth elements in minerals or rocks have been applied to the dating of minerals, the correlation of sedimentary basin rocks, the inference of marine paleochemistry, and the distinction of the biological and abiotic genesis of minerals [3–6]. Apatite is widely distributed in all kinds of igneous rocks, metamorphic rocks and sedimentary rocks, and it contains more or less rare earth elements, up to 11.14% (RE_2O_3) [7]. REEs mainly substitutes for Ca in the apatite lattice [8–11]. Benefit from its concentrations equal to or even higher than any known resource and fewer environmental concerns, REEs resource in apatite may provide a new solution to solve the global rare earth crisis [9,12].

Previous studies on rare earth elements in apatite mainly focused on the geochemical characteristics of the deposit [13–15]. Experts imply REE compositions in granular apatite are not easily altered during later burial and diagenesis [10,16–19]. However, more and more studies suggest that hydrothermal fluid will affect REE distribution in apatite during the long mineralization process [1,20–25]. Diffusion, as the basic geochemical behavior of elements, directly restricts the temporal and spatial scales of the migration of trace elements and their isotopes between mineral particles and surrounding media and is the basis of quantitative evaluation of mineral sealing to elements. Therefore, it is necessary to find out the diffusion behavior of REE in related minerals. Few experiments on interaction between REE and minerals (REE almandine, fluorite, diopside, zircon, etc.) mainly carried out

under dry conditions, which cannot be applied to the complex geological and metallogenic environment [26–29].

Apatite can accommodate any trivalent rare earth elements and has no apparent selectivity for these rare earth elements, which indicates that apatite is an arbitrary type of rare earth mineral [27,28]. Therefore, our water–mineral reaction experiments can represent the whole distribution of rare earth elements as long as it is carried out for La. In this study, we conduct the water–mineral reaction experimental study (at 400 °C, 50 MPa and 4–16 wt %) between high lanthanum (La) content hydrothermal solution and low REE content fluorapatite. The experimental apparatus is the titanium alloy autoclave, and the experimental time is 14 days. After the experiment, the La-ICP–MS in-situ analysis and the La-ICP–MS in-situ mapping analysis were used to calibrate the changes of REE contents before and after the experiment. The purpose of this experiment is to reveal the influence of different salinities on the diffusion of rare earth elements in fluorapatite and fills the blank of experimental data, which provides a quantitative parameter for the diffusion and migration of REE in apatite under the hydrothermal condition during the long geological process.

2. Materials and Methods

2.1. Experimental Instruments and Sample Pretreatment

All the experiments and the analysis of the products were completed in the Institute of geochemistry, Chinese Academy of Sciences (Guiyang). The experimental equipment is a self-tight and external heater titanium alloy autoclave (Figure 1) designed by ourselves. The chamber is sealed by a plug and a sealing ring and then pressurized by an outer nut. An external resistance furnace heats the temperature. The pressure is generated by the gasification and expansion of the fluid in the kettle, read out by the pressure gauge. Fluorapatite (FAp) with low content REE from pegmatite of the Keketuohai No.3 vein was selected as the initial material. The total REE content in these apatite grains varies from 0.315 to 0.435 ppm (the specific values are listed in Supplementary Materials Table S1), and the particle size varies from 250 to 450 μm.

Figure 1. Structural drawing of titanium alloy autoclave.

Before the experiments, Analytical pure NaCl (produced by Shanghai Aladdin Biochemical Technology Co., Ltd., Shanghai, China and the CAS number is 7647-14-5) and deionized water were used to prepare NaCl-H_2O solutions with salinity varying from 4 to 16 wt %. A gold capsule carried out FAp-REE reaction experiment, and the size of the capsule was 4 mm (outer diameter) × 3.8 mm (inner diameter) × 30 mm (length). Before loading, the gold capsule was annealed with an alcohol lamp to reduce the hardness and remove the organic matter from the tube wall. After cooling, the gold capsule was immersed in dilute hydrochloric acid for 24 h to remove the influence of impurities on the capsule wall.

2.2. Experimental Process Control

The temperature is kept at 400 °C, and the pressure is 50 MPa. To ensure the apatite can fully reach the diffusion equilibrium, the experiment should last for 14 days. The initial solution of the experiment was a pure water system and H_2O-NaCl system with the concentration of 4 wt %, 8 wt %, 12 wt % and 16 wt %; the experiment numbers were La-4-1–3, La-8-1–2, La-12-1–1 and La-16-1–2. We selected 1000 ppm standard concentration of rare earth solution as the initial solution (Store in 10% wt % HCl solution, produced by Shanghai Aladdin Biochemical Technology Co., Ltd. and the CAS number is 7439-91-0).

The loading processes were as follows: Seal one end of the gold capsule with argon arc welding, then 20 mg of the initial substance was weighed and put into a gold tube, weighed and recorded, and then 180 μL of the initial substance was removed by a pipette NaCl-H_2O solution with different salinities and 20 μL rare earth solution was transferred into the gold capsule. The gold capsule was clamped with forceps and quickly sealed by argon arc welding. During the loading process, each step needs to be weighed and recorded to ensure the initial substance and initial solution quality. After the completion of loading, the gold capsule needs to be put into the bake oven for drying for 12 h (110 °C), and then take out and allow to cool. The weight of the gold capsule is weighed by the analytical balance and recorded. If the error is less than 0.5 mg, it is considered that the sample has not leaked, which means that the welding is successful and can be used for subsequent water-rock reaction experiments.

Experimental conditions and process control: for the 50 MPa and 400 °C states, the apatite water–rock experiment is first pressurized to 20 MPa, and then heated to the test temperature within 2–3 h according to a specific heating rate (temperature controller can be programmed to set the temperature), then the pressure is adjusted to the experimental pressure 50 MPa, and the constant temperature is 14 days. To keep the pressure consistent during the experimental progress, we must check it every 4 h. If there appears a pressure drop, the pressure should be compensated in time. If the pressure drop exceeds 5 MPa, the experiment will be considered a failure.

2.3. Sample Analysis after Experiment

At the end of the experiment, the autoclave was cooled by an electric fan and then quenched. After rapid quenching, take out the gold capsule from the autoclave, wash it repeatedly with deionized water, dry it in the oven at 110 °C for 1 h and weigh it with an analytical balance. A successful experiment is if the absolute error of the weight of the gold tube before and after the experiment is less than 0.5 mg. The gold capsule is centrifuged on the centrifuge for 30 min, and then the gold tube is punctured with a steel needle, and a micropipette extracts the solution; the gold capsule is planed with a blade, and the solid product is taken out, which is repeatedly cleaned with deionized water in an ultrasonic oscillator to ensure that there is no residual NaCl crystal on the mineral surface. After cleaning, the solid products were dried and separated. The larger particles were made into targets by epoxy resin and then further analyzed in laser ablation inductively coupled plasma mass spectrometry (LA-ICP–MS).

LA-ICP–MS analysis of apatite can accurately obtain the content information of trace elements in a micro area in situ. All the analysis were completed in the State Key Laboratory

of deposit geochemistry, Institute of geochemistry, Chinese Academy of Sciences (Guiyang). The instrument used is the GeoLasPro laser ablation system manufactured by a coherent company in Germany; the specific parameters are listed in Table 1. The standard values are selected from the GeoReM database (http://georem.mpch-mainz.gwdg.de/, 4 February 2021). Companies and icpmsdata completed the off-line processing of analytical data Ca [30,31]. The main differences of mapping analysis technical indexes are: laser ablation beam spot was 7 μm, energy density was 4 mJ/cm^2 and the standard sample was NIST610.

Table 1. Summary of instruments, analytical conditions and reference materials used for the LA-ICP–MS measurements.

Laser Ablation System	
Instrument	GeoLasPro 193 nm
Energy Density (J/cm^2)	10
Safety level	IIIb
Frequency (Hz)	10
Spot Size (μm)	40
Confidence level	95%
Blank time (s)	18
Denudation time (s)	50
Detection limit of REE (ppm)	0.03–0.4
ICP–MS system	Agilent 7900
Monitored isotope	^{44}Ca, ^{89}Y, ^{139}La, ^{140}Ce, ^{141}Pr, ^{146}Nd, ^{147}Sm, ^{153}Eu, ^{160}Gd, ^{159}Tb, ^{163}Dy, ^{165}Ho, ^{166}Er, ^{165}Ho, ^{166}Er, ^{169}Tm, ^{172}Yb and ^{175}Lu.
Reference material	NIST610, NIST612, NIST614 and Durago apatite

3. Results and Discussion

3.1. Experimental Result

After the experiments, at least two apatite grains (partial pictures are listed in Figure 2) of each group were selected for LA-ICP–MS analysis. The result is listed in Table 2 (The initial content before the reaction is deducted). It can be seen that under all brine systems, the content of La in apatite decreased from edge to core, which indicates that under the conditions of high temperature and high pressure, the hydrothermal solution (bearing high content of REE) will metasomatize the crystallized apatite. Due to the different shapes and sizes of mineral particles, the different erosion positions of trace elements in the micro area in situ, and the preliminary analysis, the results may have a slight error. However, the distribution of rare earth elements in minerals can be directly obtained by in-situ surface scanning of rare earth elements in mineral particles. In this study, the LA-ICP–MS mapping analysis of La in apatite after the experiment was carried out, and the results are shown in Figure 3.

Table 2. Diffusion coefficient of La in apatite (400 °C).

Samples	C_1**/ppm**	x_1**/μm**	C_2**/ppm**	x_2**/μm**	D**/m^2/s**	D**/m^2/s (AVG)**
La-4-1	3.45	160	14.58	90	3.33×10^{-15}	
La-4-2	3.06	170	8.02	100	4.67×10^{-15}	3.74×10^{-15}
La-4-3	0.2	190	0.89	130	3.24×10^{-15}	
La-8-1	0.33	230	0.44	220	4.04×10^{-15}	3.94×10^{-15}
La-8-2	15.45	200	48.72	150	3.83×10^{-15}	
La-12-1	9.07	240	31.63	170	5.88×10^{-15}	4.73×10^{-15}
La-12-2	36.71	190	252.20	100	3.58×10^{-15}	
La-16-1	2.53	240	10.09	120	3.57×10^{-15}	3.33×10^{-15}
La-16-2	0.37	240	1.20	150	2.81×10^{-15}	

AVG represents the average value.

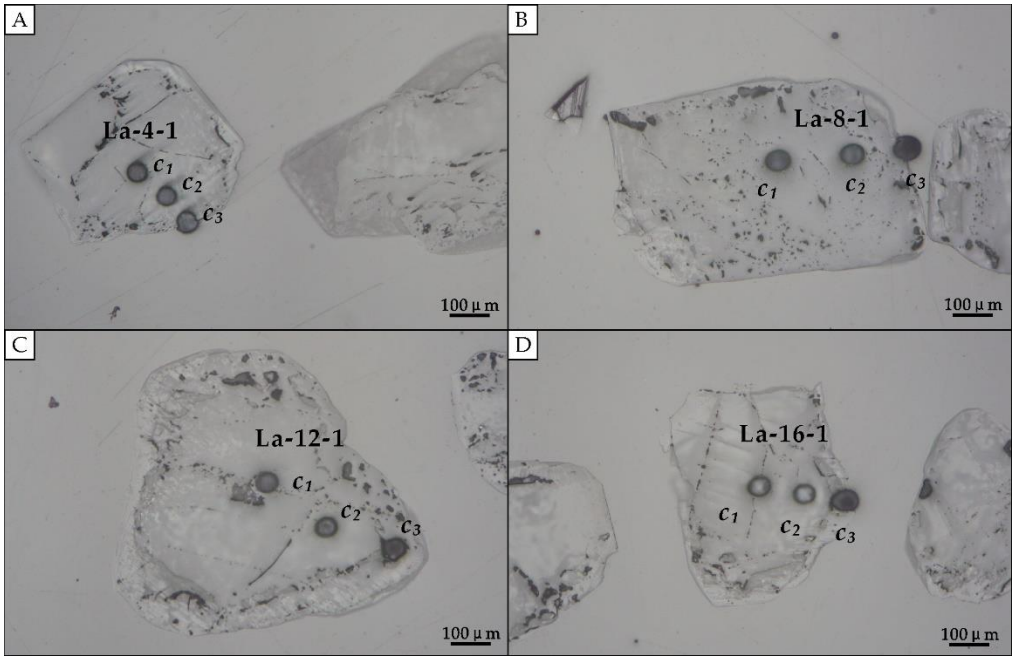

Figure 2. Location of trace element analysis in the micro area in situ. (**A**): location of La-4 grain 1, (**B**): location of La-8 grain 1, (**C**): location of La-12 grain 1, (**D**): location of La-16 grain 1.

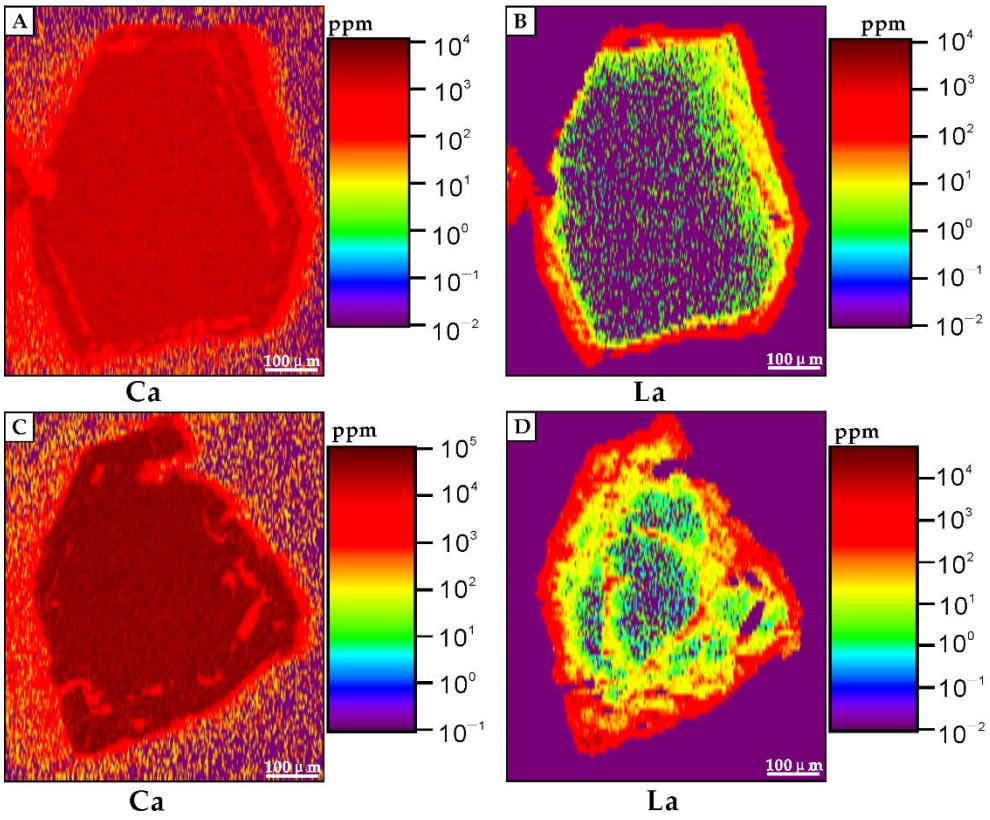

Figure 3. Mapping analyses result after water–mineral reaction (FAp-La solution). (**A**,**B**): location of La-4 grain 3, (**C**,**D**): location of La-12 grain3.

3.2. Diffusion Coefficient of La in Fluroapatite

The diffusion coefficient D and temperature T of elements in minerals obey Arrhenius law [32,33]:

$$D = D_0 \exp(-E/RT) \quad (1)$$

Or:

$$\ln D = \ln D_0 - E/RT \quad (2)$$

where D_0 (cm^2/s) is the pre-exponential factor, E (kJ/mol) is the diffusion activity energy, t (k) is the absolute temperature and R is the gas constant. According to Arrhenius law, e and d0 are constants independent of temperature and concentration, called diffusion parameters. Cherniak (2000) [34] obtained the diffusion parameters of La in fluorapatite by experiments:

$$D_{La} = 2.6 \times 10^{-7} \exp(-324 \pm 9\ \text{kJ/mol/RT})\ m^2/s \quad (3)$$

The diffusion coefficient of La is 1.69×10^{-32} m^2/s (E = 324 kJ/mol) at 400 °C (673 k). However, the initial material in this experiment is rare earth powder, and the whole experimental process is under dry conditions. REE–apatite interaction experiment is carried out in the hydrothermal system (0.28 M HCl) in this study. Generally, the diffusion of minerals in the hydrothermal system is affected by the solubility of minerals. The higher the solubility of minerals, the more conducive to the diffusion and migration of elements to the mineral centre. Therefore, the diffusion coefficient of elements in a hydrothermal system is much larger than that in a dry environment. Since there was no interaction experiment between rare earth bearing hydrothermal solution and apatite, there was no diffusion data in the hydrothermal system.

By using the element mineral internal diffusion experiment, it can be simulated as the diffusion of elements from a constant concentration source to a semi-infinite medium [34]:

$$C(x,t) = C_0\left(1 - erf\left(\frac{x}{\sqrt{4Dt}}\right)\right) \quad (4)$$

$C(x, t)$ is the distance x and time t, C_0 is the concentration of elements on the mineral surface and D is the diffusion coefficient. By substituting the experimental data into equation 6.4, the diffusion coefficient of REE in apatite at 400 °C can be obtained. Due to the dissolution and recrystallization of the mineral surface, the original mineral boundary structure may be destroyed, so we substituted the two points (C_1 and C_2) of the mineral core position to calculate the diffusion coefficient D. According to the calculation results, the diffusion coefficients of La at 400 °C were between 3.24×10^{-15} and 5.88×10^{-15} m^2/s. The trend chart of these data under different salinity conditions is shown in Figure 4.

3.3. Geological Implications

Apatite is an important carrier of rare earth elements, and the REE content in some phosphorites can be as high as 18,000 ppm [9]. However, the influence of hydrothermal fluids on the migration and enrichment of REE in apatite remains controversial. Martin and Scher (2004) [16] suggested that REE compositions are not easily altered during later burial and diagenesis. Zhu's (2017) [35] study also shows that REE enrichment in apatite occurs only in the early stage of diagenesis, and the late hydrothermal solution may have little contribution to REE content in apatite. However, many experts indicate that the hydrothermal process plays an important role in the migration and enrichment of REE in minerals [20–25].

From the LA-ICP–MS mapping analysis (Figure 3), clearly shows that the content of La decreased from the edge to the core of mineral particles, indicating hydrothermal solution can change the REE distribution in apatite. According to Figure 4, it can be seen that with the increase of salinity, the diffusion coefficient of La in apatite increased, reached the maximum at 12 wt % and then decreased. The results show that in a specific range of salinity, the rise of salinity was conducive to the diffusion of La in apatite, which may be related to the increase of mineral solubility caused by the growth of salinity. Kusebauch's

(2015) [29] experiment shows that the increase of NaCl in the initial solution will lead to the consumption of OH^- in the fluid, resulting in the decrease of pH, while Köhler (2005) [36] suggests that low pH is conducive to the dissolution of apatite and the migration of REE. NaCl is a common component in hydrothermal fluids.

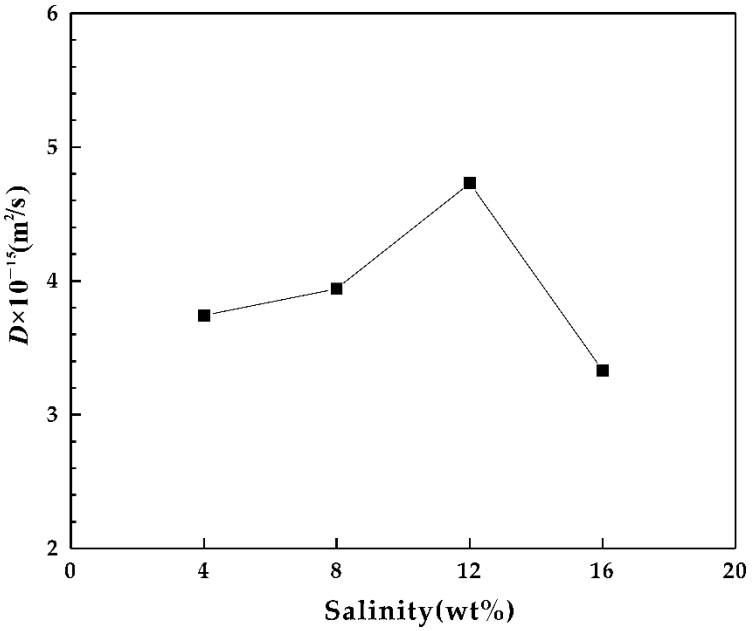

Figure 4. Trend chart of the diffusion coefficient and salinity.

4. Conclusions

The diffusion coefficients of La in fluorapatite (at 400 °C and 4–16 wt %) were between 3.24×10^{-15} and 5.88×10^{-15} m^2/s. With the increase of salinity, the diffusion coefficient of La in apatite increased, reached the maximum at 12 wt % and then decreased. The rise of salinity is conducive to the diffusion of La in apatite, which may be related to the increase of mineral solubility caused by the growth of salinity.

Although our study obtains little data on the water–mineral reaction and lacked a broader range of salinity and temperature conditions, the limited data can still enrich water–mineral experimental data, which provides a quantitative parameter for the diffusion and migration of REE in apatite under the hydrothermal condition during the long geological process. In addition, according to our experimental results, the relative migration ability of REE in apatite can be calibrated by the change of salinity within a certain range

Supplementary Materials: The following are available online at https://www.mdpi.com/article/10.3390/separations8060072/s1, Table S1: Content of rare earth elements in the microregion of apatite particles (KP03-410, ppm).

Author Contributions: Conceptualization, X.L. and H.Z.; methodology, Y.L.; investigation, X.L.; writing—original draft preparation, X.L.; writing—review and editing, H.Z. All authors have read and agreed to the published version of the manuscript.

Funding: This work was financially supported by the National Science Foundation of China (Grants Nos. 92062221) and CAS IIT (Grants Nos. JCTD-2019-17).

Conflicts of Interest: The authors declare no conflict of interest.

References

1. Smith, M.; Henderson, P.; Campbell, L. Fractionation of the REE during hydrothermal processes: Constraints from the Bayan Obo Fe-REE-Nb deposit, Inner Mongolia, China. *Geochim. Cosmochim. Acta* **2000**, *64*, 3141–3160. [CrossRef]
2. Harlov, D.E.; Förster, H.-J. Fluid-induced nucleation of (Y+REE)-phosphate minerals within apatite: Nature and experiment. Part II. Fluorapatite. *Am. Mineral.* **2004**, *88*, 1209–1229. [CrossRef]
3. Reynard, B.; Lecuyer, C.; Grandjean, P. Crystal-chemical controls on rare-earth element concentrations in fossil biogenic apatites and implications for paleoenvironmental reconstructions. *Chem. Geol.* **1999**, *155*, 233–241. [CrossRef]
4. Sano, Y.; Terada, K.; Takahashi, Y.; Nutman, A.P. Origin of life from apatite dating? *Nature* **1999**, *400*, 127–128. [CrossRef] [PubMed]
5. Bouch, J.E.; Hole, M.J.; Trewin, N.H.; Chenery, S.; Morton, A.C. Authigenic Apatite in a Fluvial Sandstone Sequence: Evidence for Rare-Earth Element Mobility During Diagenesis and a Tool for Diagenetic Correlation. *J. Sediment. Res.* **2002**, *72*, 59–67. [CrossRef]
6. Ehrenberg, S.N.; Nadeau, P.H. Postdepositional Sm/Nd Fractionation in Sandstones: Implications for Neodymium-Isotope Stratigraphy. *J. Sediment. Res.* **2002**, *72*, 304–315. [CrossRef]
7. Puchelt, H.; Emmermann, R. Bearing of rare earth patterns of apatites from igneous and metamorphic rocks. *Earth Planet. Sci. Lett.* **1976**, *31*, 279–286. [CrossRef]
8. Liu, X.; Zhang, H.; Tang, Y.; Liu, Y. REE Geochemical Characteristic of Apatite: Implications for Ore Genesis of the Zhijin Phosphorite. *Minerals* **2020**, *10*, 12. [CrossRef]
9. Emsbo, P.; McLaughlin, P.I.; Breit, G.N.; du Bray, E.A.; Koenig, A.E. Rare earth elements in sedimentary phosphate deposits: Solution to the global REE crisis? *Gondwana Res.* **2015**, *27*, 776–785. [CrossRef]
10. Jarvis, I. Phosphorite geochemistry: State-of-the-art and environmental concerns. *Eclogae Geol. Helv.* **1995**, *87*, 643–700.
11. Piper, D.Z. *Trace Elements and Major-Element Oxides in the Phosphoria Formation at Enoch Valley, Idaho Permian Sources and Current Reactivities1*; No. 99-163; U.S. Geological Survey: Reston, VA, USA, 1999.
12. Long, K.R.; Van Gosen, B.S.; Foley, N.K.; Cordier, D. The Principal Rare Earth Elements Deposits of the United States: A Summary of Domestic Deposits and a Global Perspective. In *Non-Renewable Resource Issues*; Springer: Dordrecht, The Netherlands, 2012; pp. 131–155. [CrossRef]
13. Joosu, L.; Lepland, A.; Kirsimäe, K.; Romashkin, A.E.; Roberts, N.M.W.; Martin, A.P. The REE-composition and petrography of apatite in 2 Ga Zaonega Formation, Russia: The environmental setting for phosphogenesis. *Chem. Geol.* **2015**, *395*, 88–107. [CrossRef]
14. Wright, J.; Seymour, R.S.; Shaw, H.F.; Clark, D.L. REE and Nd isotopes in conodont apatite: Variations with geological age and depositional environment. *Spec. Pap. Geol. Soc. Am.* **1984**, *196*, 325–340.
15. Morad, S. Identification of primary Ce-anomaly signatures in fossil biogenic apatite: Implication for the Cambrian oceanic anoxia and phosphogenesis. *Sediment. Geol.* **2001**, *143*, 259–264. [CrossRef]
16. Martin, E.E.; Scher, H.D. Preservation of seawater Sr and Nd isotopes in fossil fish teeth: Bad news and good news. *Earth. Planet. Sci. Lett.* **2004**, *220*, 25–39. [CrossRef]
17. Ilyin, A.V. Rare-earth geochemistry of 'old' phosphorites and probability of syngenetic precipitation and accumulation of phosphate. *Chem. Geol.* **1998**, *144*, 243–256. [CrossRef]
18. Shields, G.; Stille, P. Diagenetic constraints on the use of cerium anomalies as palaeoseawater redox proxies: An isotopic and REE study of Cambrian phosphorites. *Chem. Geol.* **2001**, *175*, 29–48. [CrossRef]
19. Shields, G.A.; Webb, G.E. Has the REE composition of seawater changed over geological time? *Chem. Geol.* **2004**, *204*, 103–107. [CrossRef]
20. Slaby, E.; Gros, K.; Förster, H.-J.; Wudarska, A.; Birski, Ł.; Hamada, M.; Götze, J.; Martin, H.; Jayananda, M.; Moyen, J.-F. Mineral–fluid interactions in the late Archean Closepet granite batholith, Dharwar Craton, southern India. *Geol. Soc. Lond. Spec. Publ.* **2019**, *489*, 293–314. [CrossRef]
21. Bouzari, F.; Hart, C.; Bissig, T.; Barker, S. Hydrothermal Alteration Revealed by Apatite Luminescence and Chemistry: A Potential Indicator Mineral for Exploring Covered Porphyry Copper Deposits. *Econ. Geol.* **2016**, *111*, 1397–1410. [CrossRef]
22. Krneta, S.; Ciobanu, C.L.; Cook, N.J.; Ehrig, K.; Kontonikas-Charos, A. Rare Earth Element Behaviour in Apatite from the Olympic Dam Cu–U–Au–Ag Deposit, South Australia. *Minerals* **2017**, *7*, 135. [CrossRef]
23. Mercer, C.N.; Watts, K.E.; Gross, J. Apatite trace element geochemistry and cathodoluminescent textures—A comparison between regional magmatism and the Pea Ridge IOAREE and Boss IOCG deposits, southeastern Missouri iron metallogenic province, USA. *Ore Geol. Rev.* **2020**, *116*, 103129. [CrossRef]
24. Li, X.; Zhou, M.-F. Multiple stages of hydrothermal REE remobilization recorded in fluorapatite in the Paleoproterozoic Yinachang Fe–Cu–(REE) deposit, Southwest China. *Geochim. Cosmochim. Acta* **2015**, *166*, 53–73. [CrossRef]
25. Gros, K.; Słaby, E.; Förster, H.-J.; Michalak, P.P.; Munnik, F.; Götze, J.; Rhede, D. Visualization of trace-element zoning in fluorapatite using BSE and CL imaging, and EPMA and μPIXE/μPIGE mapping. *Mineral. Petrol.* **2016**, *110*, 809–821. [CrossRef]
26. Orman, J.; Grove, T.L.; Shimizu, N. Rare earth element diffusion in diopside: Influence of temperature, pressure, and ionic radius, and an elastic model for diffusion in silicates. *Contrib. Mineral. Petrol.* **2001**, *141*, 687–703. [CrossRef]
27. Harrison, W.J.; Wood, B.J. An experimental investigation of the partitioning of REE between garnet and liquid with reference to the role of defect equilibria. *Contrib. Mineral. Petrol.* **1980**, *72*, 145–155. [CrossRef]

28. Ganguly, J.; Tirone, M.; Hervig, R. Diffusion kinetics of samarium and neodymium in garnet, and a method for determining cooling rates of rocks. *Science* **1998**, *281*, 805–807. [CrossRef] [PubMed]
29. Kusebauch, C.; John, T.; Whitehouse, M.J.; Klemme, S.; Putnis, A. Distribution of halogens between fluid and apatite during fluid-mediated replacement processes. *Geochim. Cosmochim. Acta* **2015**, *170*, 225–246. [CrossRef]
30. Liu, Y.S.; Hu, Z.C.; Zong, K.Q.; Gao, C.G.; Chen, H.H. Reappraisement and refinement of zircon U-Pb isotope and trace element analyses by LA-ICP-MS. *Chin. Sci. Bull.* **2010**, *55*, 1535–1546. [CrossRef]
31. Zhou, L.; Mernagh, T.P.; Lan, T.; Tang, Y.; Wygralak, A. Intrusion related gold deposits in the Tanami and Kurundi-Kurinelli goldfields, Northern Territory, Australia: Constraints from LA-ICPMS analysis of fluid inclusions. *Ore Geol. Rev.* **2019**, *115*. [CrossRef]
32. Freer, R. Diffusion in silicate minerals and glasses: A data digest and guide to the literature. *Contrib. Mineral. Petrol.* **1981**, *76*, 440–454. [CrossRef]
33. Dodson, M.H. Closure temperature in cooling geochronological and petrological systems. *Contrib. Mineral. Petrol.* **1973**, *40*, 259–274. [CrossRef]
34. Cherniak, D. Rare earth element diffusion in apatite. *Geochim. Cosmochim. Acta* **2000**, *64*, 3871–3885. [CrossRef]
35. Zhu, B.I.; Jiang, S.-Y. A LA-ICP-MS analysis of rare earth elements on phosphatic grains of the Ediacaran Doushantuo phosphorite at Weng'an, South China: Implication for depositional conditions and diagenetic processes. *Geol. Mag.* **2017**, *154*, 1381–1397. [CrossRef]
36. Köhler, S.J.; Harouiya, N.; Chaïrat, C.; Oelkers, E.H. Experimental studies of REE fractionation during water–mineral interactions: REE release rates during apatite dissolution from pH 2.8 to 9.2. *Chem. Geol.* **2005**, *222*, 168–182. [CrossRef]